Detection Probability of Harmonics in Power Systems Affected by Frequency Fluctuation

Diego Bellan

***Abstract*—**This paper deals with the analytical derivation of detection probability of power system harmonics affected by frequency instability. Indeed, when the number of data samples is small in order to limit the computational burden (e.g., in continuous real-time monitoring of voltage/current spectra for power quality purposes), contribution of additive noise reduces significantly the detection probability of harmonics in the discrete Fourier transform domain. If the waveform is affected by frequency instability (emphasized for higher order harmonics), the lack of synchronism between harmonics and sampling frequencies results in a further reduction of detection probability due to the attenuation effect introduced by the window used against spectral leakage. The analytical model derived in the paper takes into account both additive noise and frequency instability to the aim of evaluating detection probability of harmonics. Analytical results are validated by means of numerical simulations.

***Keywords*—**Additive noise, discrete Fourier transform, Harmonic analysis, time-varying frequency.

I. Introduction

CONTINUOUS real-time monitoring of frequency spectra of voltage and current waveforms is an important issue in modern power systems characterized by a widespread use of nonlinear and switched loads and sources [1]-[2]. In general terms, digital techniques are well-suited to the purpose of spectra evaluations since many sophisticated algorithms have been proposed in the technical literature for processing waveforms affected by critical characteristics such as time-varying frequency or amplitude [3]-[4]. However, the use of sophisticated algorithms contrasts with the need of continuous real-time monitoring because of the requested computational burden. Typically, computational burden can be controlled by limiting the number of samples in each waveform acquisition for analog-to-digital (A/D) and time-to-frequency conversion through the discrete Fourier transform (DFT). It is well known that the main drawback of a small number of acquisition samples is to emphasize the impact of additive noise always present in electrical measurements. High noise levels in the frequency domain can result in the lack of detection of harmonic components in the waveform under analysis. This phenomenon is further emphasized in the case of waveforms affected by time-varying frequency (or frequency instability) because the lack of synchronism between the waveform harmonics and the sampling frequency results in underestimation of the measured harmonic amplitude [4]. Even in the case of a closed-loop measurement system [1] the phenomenon can be significant since a small frequency instability in the waveform fundamental frequency is magnified by the harmonic order, and therefore significant effects can be observed for high-order low-amplitude harmonics.

In the literature, the detection probability of a sine wave in additive noise in the frequency domain has been already investigated [5], but the effect of the lack of synchronism has not been investigated analytically as far as probability of detection is concerned. In fact, only the worst case was considered, i.e., the case of a sine wave component with frequency in the middle point between two adjacent frequency bins [6]-[7]. Therefore, the detection probability of a sine wave in additive noise taking into account its frequency instability in analytical terms is the main objective of this paper.

In this work, frequency instability of harmonic components is modeled as a uniformly distributed random variable. An approximate analytical representation is introduced for the attenuation effect of window functions used against spectral leakage [8]. As a result, random behavior of harmonic frequency is included in the analytical derivation of the detection probability taking into account both additive noise and frequency instability effects.

The paper is organized as follows. In Section II the problem statement is presented. In Section III the approximate analytical model for the frequency instability effects on the measured harmonic magnitude is introduced. In Section IV the conventional model for the detection probability in additive noise is extended to include the probabilistic model of frequency instability effects. In Section V the analytical results derived in the previous Sections are validated by means of numerical simulations. Concluding remarks are reported in Section VI.

II. Problem Statement

Measurement of power system harmonics can be effectively performed by resorting to digital instrumentation based on A/D conversion of voltage and current waveforms, and time-to-frequency transformation through the DFT (with the efficient FFT algorithm) [7], [9]-[10]. Thus, harmonics magnitude at each frequency of interest can be readily evaluated by reading the amplitude of the relevant spectral lines.

D. Bellan is with the Department of Electronics, Information and Bioengineering, Politecnico di Milano, 20133 Milan, Italy (phone: +39-02-23993708; fax: +39-02-23993703; e-mail: diego.bellan@polimi.it).

Two main sources of uncertainty can be identified in the measurement process outlined above. First, the fundamental frequency of voltage/current waveforms is typically affected by random instability. It means that by repeating the measurement process, slightly different values of the waveforms fundamental frequency must be expected. Such frequency instability is of course emphasized for harmonic components. When the DFT is applied, the lack of synchronism between the frequency of the waveform sinusoidal components and the sampling frequency (i.e., non-coherent sampling) will result in increased uncertainty in the amplitude measurements [6], [8]. The second main source of uncertainty is additive noise. Indeed, voltage/current waveforms are always affected by additive noise which propagates through A/D conversion and DFT transformation, yielding noisy spectral lines. It is expected that the impact of additive noise is larger as the amplitude of the involved harmonic spectral lines decreases. Spectral effects of additive noise have been investigated in many previous papers (e.g., [7]-[13]).

The time-domain voltage waveform is modelled as a sum of *N* harmonically related sine waves and zero-mean white Gaussian noise:

$$v(t) = \sum_{h=1}^{N} V_h \cos(2\pi h f_0 t + \varphi_h) + n(t) \qquad (1)$$

A similar expression holds for the current waveform, therefore in this paper mathematical derivations will be presented for the voltage waveform only.

After A/D conversion of (1) with sampling frequency f_s, and weighted time-windowing (N_S samples in length) against spectral leakage [6]-[8], the DFT transform provides the estimates of the complex Fourier coefficients:

$$\hat{V}_n = \frac{2}{N_S \mathrm{NPSG}} \sum_{k=0}^{N_S-1} v[k] w[k] \exp(-j2\pi kn/N_S), \qquad (2)$$

where $w[k]$ is the selected time window characterized by the related Normalized Peak Signal Gain NPSG (see Tab. I where three examples of commonly used windows are reported with the parameters exploited in this paper). The frequency index *n* is related to the frequency index *h* in (1) by $n \times \Delta f = h \times f_0$, where $\Delta f = f_s/N_s$ is the DFT frequency resolution. Under non-coherent sampling, the relation $n \times \Delta f = h \times f_0$ is intended as an approximate relation where *n* is the index such that $n \times \Delta f$ is the discrete frequency closest to $f_h = h \times f_0$.

In the next Section the statistical properties of $|\hat{V}_n|$ will be derived as functions of the statistical properties of f_h treated as a random variable (RV). The subscripts *n* and *h* will be dropped since the derivations hold for any frequency index.

III. Mathematical Modeling of Frequency Instability Effects

In this Section only the effects of frequency instability are investigated. Additive noise effects will be described in Section IV.

If the frequency *f* of a harmonic component in the voltage waveform does not equal one of the DFT discrete frequencies (i.e., the integer multiples of the frequency resolution Δf), the related spectral-line magnitude does not take its ideal value. In fact, in this case (i.e., the non-coherent sampling condition) the spectral line magnitude is weighted by the Fourier transform of the time window $w[k]$ used in (2) against spectral leakage. An approximate methodology is here introduced, consisting in the approximation of the frequency-domain behavior of each specific window by a parabolic function obtained by setting the constraint provided by the window Scallop Loss (SL) (see Fig. 1), i.e., the maximum attenuation introduced by the window at the edges $\pm \Delta f/2$ of each DFT bin [6]. From Fig. 1, assuming the *n*-th DFT frequency bin as the origin of the frequency axis, the attenuation introduced by the window on a waveform spectral line can be readily obtained [8]:

$$y \cong 1 - \frac{4(1-SL)}{\Delta f^2} f^2 \qquad (3)$$

Such attenuation is applied to the actual amplitude *V* of each sinusoidal component in (1). Therefore, the measured amplitude of each sinusoidal component can be written:

$$M = yV \qquad (4)$$

where *V* denotes the non-weighted frequency-centered spectral line.

The frequency f will be treated as a RV uniformly distributed within an interval $\delta f < \Delta f$ centered on the DFT frequency bin $n \times \Delta f$ (see Fig. 1). Thus, the probability density function (PDF) of the frequency is $1/\delta f$ within the interval $\pm \delta f/2$. It follows that also *y* is a RV whose mean value and variance can be evaluated analytically in a straightforward way [14]:

$$\mu_y = \int_{\frac{-\delta f}{2}}^{\frac{+\delta f}{2}} y \frac{1}{\delta f} df = 1 - \frac{1}{3}(1-SL)\left(\frac{\delta f}{\Delta f}\right)^2 \qquad (5)$$

$$\sigma_y^2 = \int_{\frac{-\delta f}{2}}^{\frac{+\delta f}{2}} (y-\mu_y)^2 \frac{1}{\delta f} df = \frac{4}{45}(1-SL)^2 \left(\frac{\delta f}{\Delta f}\right)^4 \qquad (6)$$

The cumulative distribution function (CDF) of the RV *y* can be readily evaluated by considering that for a given value *y* the corresponding values of *f* can be obtained by inversion of (3) as

$$f_{1,2} = \pm \sqrt{\frac{1-y}{4(1-SL)}} \qquad (7)$$

Therefore, the CDF of the RV *y* is given by:

$$F_y(y) = 1 - \frac{\Delta f}{\delta f} \sqrt{\frac{1-y}{1-SL}} \qquad (8)$$

The PDF of the RV *y* can be readily obtained from (8) by derivation:

$$f_y(y) = \frac{dF_y}{dy} = \frac{\Delta f}{2\delta f \sqrt{(1-y)(1-SL)}} \qquad (9)$$

Finally, by taking into account (4), the following analytical results hold for the measured harmonic amplitude [14]:

$$\mu_M = \mu_y V \tag{10}$$

$$\sigma_M^2 = \sigma_y^2 V^2 \tag{11}$$

$$F_M(M) = 1 - \frac{\Delta f}{\delta f}\sqrt{\frac{1-\frac{M}{V}}{1-SL}} \tag{12}$$

$$f_M(M) = \frac{1}{V}\frac{\Delta f}{2\delta f\sqrt{\left(1-\frac{M}{V}\right)(1-SL)}} \tag{13}$$

IV. Detection Probability Taking Into Account Frequency Instability and Additive Noise

A. Background on Detection Probability

Additive noise $n(t)$ in (1) results in a random behavior of the DFT coefficients $\hat{V}_n$ in (2). The real and the imaginary parts of each $\hat{V}_n$ can be approximated as a Gaussian RV with unbiased mean value (i.e., the deterministic noise-free values), and variance [9]-[13], [15]

$$\sigma^2 = ENBW\frac{2}{N_S}\sigma_n^2 \tag{14}$$

where ENBW is the equivalent noise bandwidth of the selected window $w(t)$, and σ_n^2 is the variance of the input noise $n(t)$. As a result, the only-noise spectral lines (i.e., with zero deterministic component) have a Rayleigh probability density function (PDF) [7], [9]-[13]:

$$g_{|\hat{V}|}\left(|\hat{V}|\right) = \frac{|\hat{V}|}{\sigma^2}\exp\left(-\frac{|\hat{V}|^2}{2\sigma^2}\right) \tag{15}$$

and cumulative distribution function (CDF):

$$G_{|\hat{V}|}\left(|\hat{V}|\right) = 1 - \exp\left(-\frac{|\hat{V}|^2}{2\sigma^2}\right) \tag{16}$$

Notice that in (15) and (16) the frequency subscript n was dropped since the results are independent of n.

On the other hand, the signal spectral lines (i.e., with non-zero deterministic component) have Rician PDF [9]-[13], [16]:

$$f_{|\hat{V}|}\left(|\hat{V}|\right) = \frac{|\hat{V}|}{\sigma^2}\exp\left(-\frac{|\hat{V}|^2+M^2}{2\sigma^2}\right)I_0\left(\frac{|\hat{V}|M}{\sigma^2}\right) \tag{17}$$

TABLE I.
SOME FIGURES OF MERIT OF THREE COMMON WINDOWS.

Window	NPSG	ENBW	SL [dB]	SL
Rect.	1	1	3.92	0.637
Tukey (α=0.5)	0.75	1.22	2.24	0.773
Hann	0.50	1.50	1.42	0.849

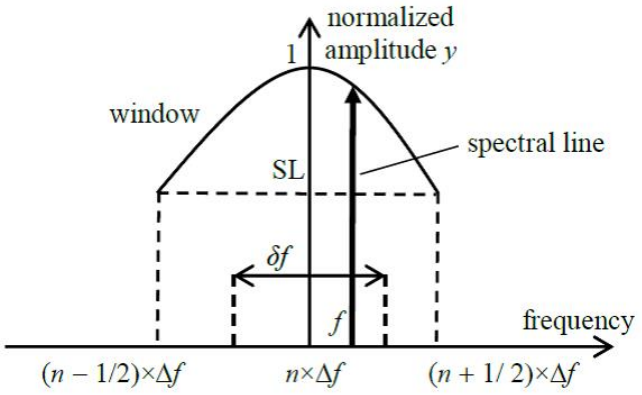

Fig. 1. Spectral line weighted by the frequency-domain window.

where M is the related sine wave amplitude weighted by the spectrum of the window $w(t)$ (see (4)), and I_0 is the modified Bessel function of the first kind. If the considered sine wave frequency equals an integer multiple of Δf than the weight introduced by the window spectrum is equal to one, otherwise the weight is less than one. The CDF is given by

$$F_{|\hat{V}|}\left(|\hat{V}|\right) = 1 - Q_1\left(\frac{M}{\sigma}, \frac{|\hat{V}|}{\sigma}\right) \tag{18}$$

where Q_1 is the Marcum Q function.

By defining a threshold level α, the false alarm probability is defined as the probability that an only-noise spectral line is larger than α. Thus, from (16) the false alarm probability is given by

$$P_{fa}(\alpha) = \exp\left(-\frac{\alpha^2}{2\sigma^2}\right) \tag{19}$$

The detection probability is defined as the probability that a signal spectral line is greater than the threshold. Thus, from (18) the detection probability is given by

$$P_d(\alpha) = Q_1\left(\frac{M}{\sigma}, \frac{\alpha}{\sigma}\right) \tag{20}$$

By solving (19) with respect to α and substituting into (20) we obtain [5]

$$P_d\left(P_{fa}\right) = Q_1\left(\frac{M}{\sigma}, \sqrt{-2\log\left(P_{fa}\right)}\right) \tag{21}$$

Therefore, for a given signal-to-noise ratio M/σ, eq. (21) provides the detection probability as a function of the accepted false alarm probability.

B. Impact of Frequency Instability on Detection Probability

The measured amplitude of a harmonic spectral line is affected by both additive noise and frequency fluctuation. Therefore, the detection probability for a given threshold level α must be obtained from the total probability theorem by

combining (20) (representing only the noise contribution for a given harmonic amplitude M) and (13) (representing the frequency fluctuation contribution) [14]:

$$P_d(\alpha) = \int_{SL\cdot V}^{V} P_d(\alpha|M) f_M(M) dM =$$

$$= \int_{SL\cdot V}^{V} Q_1\left(\frac{M}{\sigma}, \frac{\alpha}{\sigma}\right) f_M(M) dM \qquad (22)$$

and by taking into account (4) we obtain:

$$P_d(\alpha) = \int_{SL}^{1} Q_1\left(SNR \cdot y, \frac{\alpha}{\sigma}\right) f_y(y) dy \qquad (23)$$

where

$$SNR = \frac{V}{\sigma} \qquad (24)$$

is the harmonic signal-to-noise ratio.

Finally, by taking into account (19), the detection probability can be expressed as a function of the false alarm probability as

$$P_d(P_{fa}) = \int_{SL}^{1} Q_1\left(SNR \cdot y, \sqrt{-2\log(P_{fa})}\right) f_y(y) dy \qquad (25)$$

V. Numerical Validation

The analytical results derived in Sections III and IV have been validated by resorting to numerical simulation of the whole measurement process. According to (1), a voltage waveform consisting of three harmonic components was selected such that $f_0 = 50$ Hz, and $h = 1, 3, 5$. The harmonic amplitudes were selected as $V_1 = 10, V_3 = 2, V_5 = 1$. Phase angles were selected at random. Sampling was performed such that 10 periods of the fundamental component were acquired, i.e., a 200 ms measurement window were taken. The selection of the number of samples N_s defines the corresponding sampling frequency. By assuming $N_s = 2^{12}$ the corresponding sampling frequency was $f_s = 20.48$ kHz, and the related frequency resolution was $\Delta f = 5$ Hz. A repeated run analysis (10^4 runs to estimate each average value) was performed by assuming f_0 taking random values with uniform distribution within a frequency range δf centered on the nominal frequency 50 Hz [17]-[18]. It is worth noticing that a frequency deviation δf in the fundamental component results in a frequency deviation $3\delta f$ in the third harmonic, and $5\delta f$ in the fifth harmonic. In the following, analytical results were validated for the fifth harmonic. In fact, by assuming a maximum $\frac{\delta f}{\Delta f} = 0.2$ for the fundamental component, such normalized frequency range equals 1 for the fifth harmonic.

In Fig. 2 the numerical estimates (dotted lines) of the mean value of the fifth harmonic amplitude are compared with the analytical result (10) (solid lines). The three different windows considered in Tab. I were used. Clearly the rectangular window shows the worst behavior due to its lowest SL value.

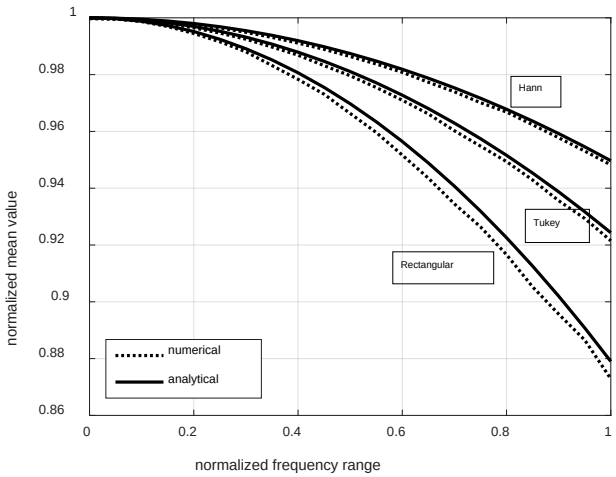

Fig. 2. Comparison between analytical (solid lines) and numerical (dotted lines) mean value of the amplitude of the fifth harmonic as a function of the normalized frequency range $\delta f/\Delta f$ due to frequency instability, for three different windows.

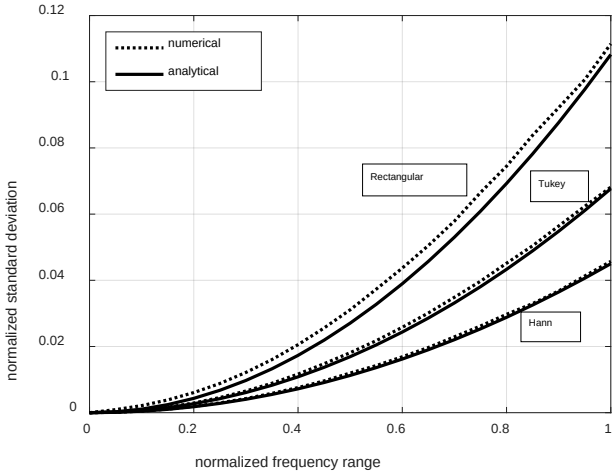

Fig. 3. Comparison between analytical (solid lines) and numerical (dotted lines) estimates of the normalized standard deviation of the amplitude of the fifth harmonic as a function of the normalized frequency range $\delta f/\Delta f$ due to frequency instability, for three different windows.

In Fig. 3 the numerical estimates (dotted lines) of the standard deviation of the fifth harmonic amplitude are compared with the analytical results given by the square root of (11) (solid lines).
Also in this case the best behavior is provided by the Hann window due to its larger SL.

Fig. 4 shows the behavior of the detection probability of the fifth harmonic as a function of the false alarm probability in the case of rectangular window and additive Gaussian noise such that SNR as defined in (24) for the fifth harmonic is equal to 5. Frequency instability is such that δf for the fifth harmonic is equal to 0.5 Hz and 5 Hz (i.e., 0.1 Hz and 1 Hz for the fundamental frequency f_0, respectively). Dotted lines refer to numerical results whereas solid lines refer to (25). Of course, larger frequency instability results in lower detection probability due to a larger attenuation effect of the window in the frequency domain. Figs. 5 and 6 show the same behavior in

the case of Tukey and Hann window, respectively. Detection probability increases with the value of SL and this is confirmed by the figures. In fact, while the curves for lower frequency instability (i.e., 0. 5 Hz) are similar for Figs. 4-6, the curves for larger frequency instability (i.e., 5 Hz) increase with SL because of the different behavior around the edges of the main lobe of the windows in the frequency domain. Figs. 7-9 are similar to Figs. 4-6 but with the fifth harmonic SNR equal to 4 instead of 5. It means that the noise level was increased. Two phenomena are expected from a higher noise level. First, the detection probabilities decrease with respect to Figs. 4-6. Second, it is expected a lower influence of the attenuation introduced by the windows, i.e., a lower spread between the curves in each of the Figs. 7-9. Comparison between Figs. 4-6 and Figs. 7-9 confirms both the phenomena expected from a higher noise level.

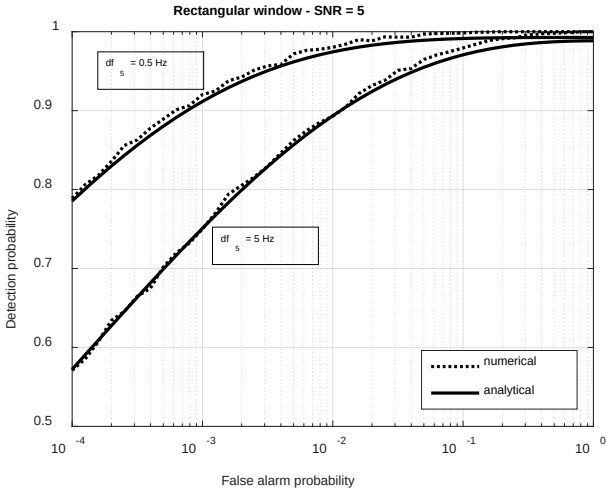

Fig. 4. Detection probability of the fifth harmonic as a function of false alarm probability using rectangular window, noise level such that SNR=5 and frequency instability δf equal to 0.5 Hz and 5 Hz for the fifth harmonic.

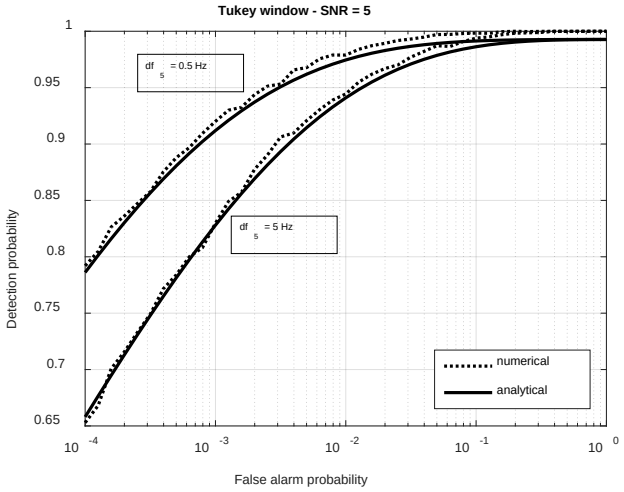

Fig. 5. Detection probability of the fifth harmonic as a function of false alarm probability using Tukey window, noise level such that SNR=5 and frequency instability δf equal to 0.5 Hz and 5 Hz for the fifth harmonic.

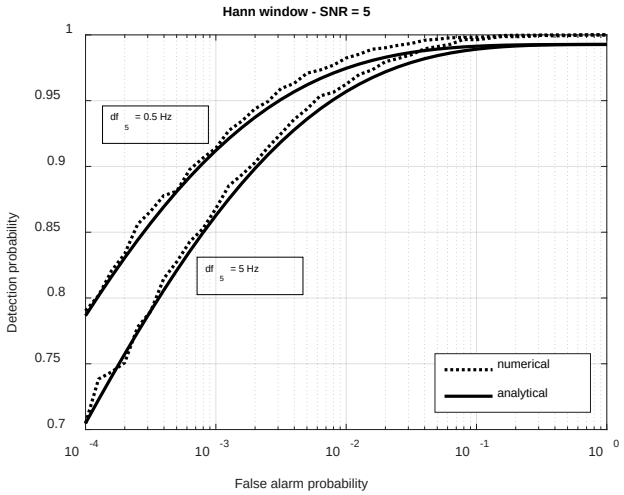

Fig. 6. Detection probability of the fifth harmonic as a function of false alarm probability using Hann window, noise level such that SNR=5 and frequency instability δf equal to 0.5 Hz and 5 Hz for the fifth harmonic.

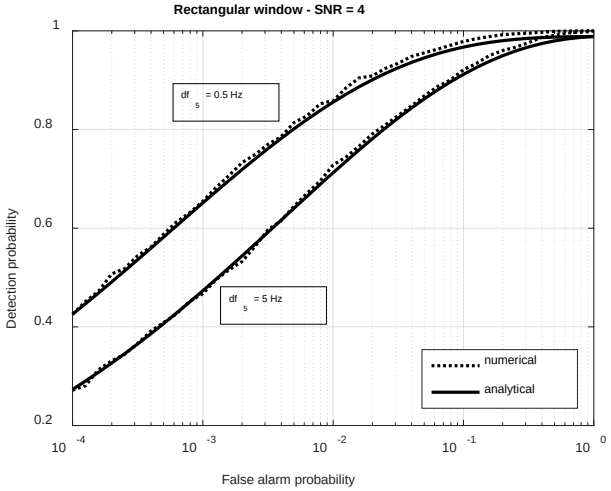

Fig. 7. Detection probability of the fifth harmonic as a function of false alarm probability using rectangular window, noise level such that SNR=4 and frequency instability δf equal to 0.5 Hz and 5 Hz for the fifth harmonic.

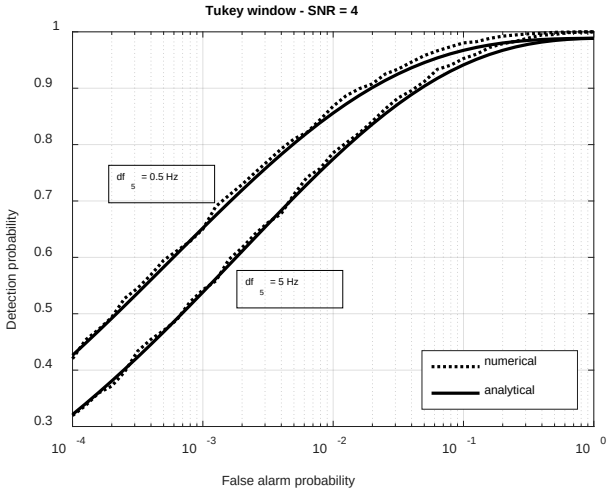

Fig. 8. Detection probability of the fifth harmonic as a function of false alarm probability using Tukey window, noise level such that SNR=4 and frequency instability δf equal to 0.5 Hz and 5 Hz for the fifth harmonic.

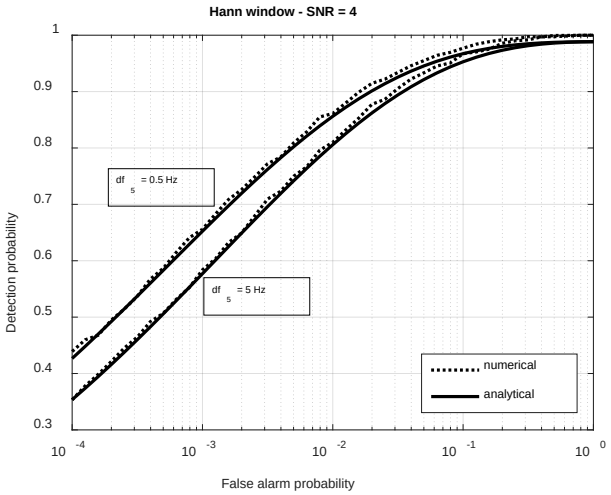

Fig. 9. Detection probability of the fifth harmonic as a function of false alarm probability using Hann window, noise level such that SNR=4 and frequency instability δf equal to 0.5 Hz and 5 Hz for the fifth harmonic.

VI. Conclusion

Analytical results derived in the paper concerning the statistical properties of the measured amplitude of harmonics affected by frequency instability have shown good agreement with numerical results. It should be highlighted that the proposed approach is an approximate approach since the frequency behavior of the window has been approximated by a parabolic behavior. The advantage of the proposed approach is its simplicity and the possibility to be used in a straightforward way for a general window by using only the scallop loss parameter of the selected window. Future work will be devoted to include in the model more general statistical distributions of the frequency instability such as a range larger than the frequency bin and possibly non-symmetrical (i.e., the case of interharmonic components).

References

[1] IEC 61000-4-7, *Electromagnetic compatibility (EMC) – Part 4-7: Testing and measurement techniques – General guide on harmonics and interharmonics measurements and instrumentation, for power supply systems and equipment connected thereto.* IEC, 2002.

[2] D. Bellan, G. Superti Furga, and S. A. Pignari, "Circuit representation of load and line asymmetries in three-phase power systems," *International Journal of Circuits, Systems and Signal Processing*, vol. 9, pp. 75-80, 2015.

[3] C. Chen and Y. Chen, "Comparative Study of Harmonic and Interharmonic Estimation Methods for Stationary and Time-Varying Signals," *IEEE Trans. on Industrial Electronics, vol. 61*, no. 1, pp. 397-404, Jan. 2014.

[4] D. Belega, D. Dallet, and D. Petri, "Accuracy of Sine Wave Frequency Estimation by Multipoint Interpolated DFT Approach," *IEEE Trans. on Instrum. Meas.*, vol. 59, no. 11, pp. 2808-2815, 2010.

[5] H.C. So, Y.T. Chan, Q. Ma, and P.C. Ching, "Comparison of various periodograms for sinusoid detection and frequency estimation," *IEEE Trans. Aerospace and Electronic Systems, vol. 35*, pp. 945-952, July 1999.

[6] F. J. Harris, "On the use of windows for harmonic analysis with the discrete Fourier transform," *Proc. of the IEEE*, vol. 66, pp. 51-83, 1978.

[7] O. M. Solomon, "The use of DFT windows in signal-to-noise ratio and harmonic distortion computations," *IEEE Trans. Instrum. Meas., vol. 43*, pp. 194-199, April 1994.

[8] D. Bellan, "Frequency Instability and Additive Noise Effects on Digital Power Measurements Under Non-Sinusoidal Conditions," in *Proc. 2014 6th IEEE Power India International Conference (PIICON)*, Delhi, India, Dec. 5-7, 2014, pp. 1-5.

[9] D. Bellan, "Statistical Characterization of Harmonic Emissions in Power Supply Systems," *International Review of Electrical Engineering*, vol. 9, no. 4, pp. 803-810, 2014.

[10] D. Bellan, "Characteristic Function of Fundamental and Harmonic Active Power in Digital Measurements Under Nonsinusoidal Conditions," *International Review of Electrical Engineering*, vol. 10, no. 4, pp. 520-527, 2015.

[11] D. Bellan, A. Gaggelli, and S. A. Pignari, "Noise Effects in Time-Domain Systems Involving Three-Axial Field Probes for the Measurement of Nonstationary Radiated Emissions," *IEEE Trans. on Electromagn. Compat.*, vol. 51, no. 2, pp. 192-203, 2009.

[12] D. Bellan, "Noise Propagation in Multiple-Input ADC-Based Measurement Systems," *Measurement Science Review*, vol. 14, no. 6, pp. 302-307, 2014.

[13] D. Bellan, "On the Validity of the Noise Model of Quantization for the Frequency-Domain Amplitude Estimation of Low-Level Sine Waves," *Metrology and Measurement Systems*, vol. 22, no. 1, pp. 89-100, 2015.

[14] A. Papoulis and S. U. Pillai, *Probability, Random Variables and Stochastic Processes*. McGraw-Hill, 4th Ed., 2002.

[15] D. Bellan and S.A. Pignari, "Statistical superposition of crosstalk effects in cable bundles," *China Communications, vol. 10*, no. 11, pp. 119-128, 2013.

[16] M. K. Simon, *Probability Distributions Involving Gaussian Random Variables.* Springer, 2002.

[17] S. A. Pignari and D. Bellan, "Incorporating vertical risers in the transmission line equations with external sources," in *Proc. 2004 IEEE International Symposium on Electromagnetic Compatibility*, Santa Clara, CA, USA, Aug. 2004, pp. 974-979.

[18] D. Bellan and S. A. Pignari, "Efficient estimation of crosstalk statistics in random wire bundles with lacing cords," *IEEE Trans. on Electromagn. Compat.*, vol. 53, pp. 209-218, Feb. 2011.